Research Article

INTERNATIONAL JOURNAL OF ADVANCED ROBOTIC SYSTEMS

International Journal of Advanced Robotic Systems
May-June 2017: 1–8

DOI: 10.1177/1729881417716634
journals.sagepub.com/home/arx
SAGE

Kinematics and dynamics analysis of a novel five-degrees-of-freedom hybrid robot

You Wu[1], Zhen Yang[1], Zhuang Fu[1], Jian Fei[2] and Hui Zheng[1]

Abstract

In this article, a novel five-degrees-of-freedom hybrid robot is proposed and its kinematics and dynamics are analyzed systematically. First, the mechanism is designed. It is composed of a traditional three-degrees-of-freedom delta robot and a two-degrees-of-freedom serial mechanism. Second, the forward kinematics is established by geometric method, and the inverse kinematics is established by Denavit-Hartenberg (D-H) matrix method. Third, based on the principle of virtual work, Lagrange equations of dynamics are deduced. Finally, the feasibility and advantage of the proposed robot are verified by simulation and experiment.

Keywords

Hybrid robot, kinematics, dynamics, ADAMS simulation, Lagrange equation

Date received: 19 September 2016; accepted: 4 March 2017

Topic: Robot Manipulation and Control
Topic Editor: Andrey V Savkin
Associate Editor: Oleg Yakimenko

Introduction

Serial robots and parallel robots are two main types of robots used in industries.[1] Serial robots are traditional robots with large workspace and high dexterity.[2] However, the stiffness of the series structure is low.[3] The speed of parallel robots is fast, and the stiffness is high. However, many parallel robots suffer from the disadvantages of difficult direct kinematics, coupled position, and small workspace.[4] Hybrid robots combined of serial robots and parallel robots are being developed in recent years.[5] This kind of robot plays an important role in spatial works such as assembly, package, and transit.

Different hybrid robots have been proposed in the literature. In 1999, Romdhane designed a six-degrees-of-freedom (DOF) hybrid serial–parallel manipulator. It was made of a base and two platforms in series.[6] In 2002, Tsai and Joshi proposed a three-DOF hybrid mechanism.[7] The mechanism consisted of a position mechanism and an orientation mechanism. Huang et al. in Tianjin University proposed a three-DOF parallel mechanism module which formed the main body of a reconfigurable hybrid robot. The well-known Tricept robot is a hybrid system with a three-DOF parallel mechanism and a two-DOF serial mechanism. The parallel part of Tricept robot is usually formed by hydraulic poles or ball screws, and thus, the mechanism of Tricept robot is huge.[8] Liang and Ceccarelli designed a waist–trunk system. The waist–trunk system consisted of a three-legged parallel platform and a six-legged parallel system. The two platforms were connected in a serial architecture. The system was designed for humanoid robots with the advantages of high payload, high stiffness, and accuracy, but the structure was too complicated.[9,10] In 1999, ABB Flexible Automation launched a four-DOF delta

[1] State Key Lab of Mechanical System and Vibration, Shanghai Jiao Tong University, Shanghai, China
[2] Ruijin Hospital Affiliated to Shanghai Jiao Tong University, Shanghai, China

Corresponding authors:
Zhuang Fu, Shanghai Jiao Tong University, 800 Dongchuan Road, Shanghai 200240, China.
Email: zhfu@sjtu.edu.cn

Jian Fei, Ruijin Hospital Affiliated to Shanghai Jiao tong University, Shanghai, China.
Email: feijian@hotmail.com

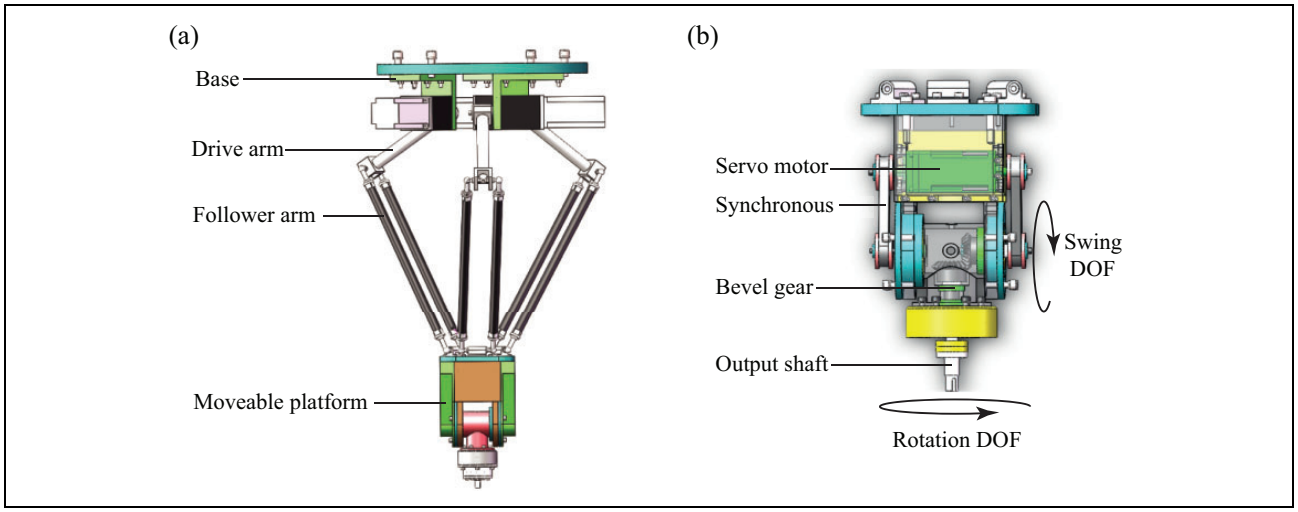

Figure 1. The architecture design of 5-DOF hybrid robot. 5-DOF: five-degrees-of-freedom.

robot under the name IRB 340 FlexPicker. Compared with traditional delta robot, the IRB robot has more flexibility and larger scope of application. FANUC Robotics developed two types of delta robots, M-1iA with four or six DOFs, and M-3iA with four or six DOFs. The FANUC delta robots offer the motion flexibility of a human wrist, fast cycle times, ultracompact arm, and precision.[11] The theories of hybrid mechanism have not found a sound system. Most hybrid robots consist of two parallel mechanisms or consist of a parallel mechanism and a serial mechanism. Delta robots are a kind of parallel robots, which are widely used in industries.[12,13] Traditional delta robots have three translational DOFs. As delta robots are getting widely used in various fields, only three DOFs can no longer meet the more complex working conditions. In this article, based on delta robot, a novel five-DOF hybrid robot is proposed. The hybrid robot is a robot with three pure translational DOFs and two rotational DOFs. The two rotational DOFs can expand the application of delta robots. The five-DOF hybrid robot will have potential application in assembly, package, and transit.

For the content of this article, the configuration of the hybrid robot is introduced in the next section. Then, the forward kinematics is derived by the geometric method, and the inverse kinematics is derived by the Denavit-Hartenberg (D-H) matrix method. The dynamic analysis is done in the following two sections. At last, experiment is done to verify the feasibility of the hybrid robot.

Mechanism design

A delta robot includes three in-paralleled limbs between a fixed frame and a platform which moves by the spherical rotation about a fixed point. For the traditional delta robot, the moving platform has only three translational DOFs; thus, the posture of the robot is strictly limited. In this

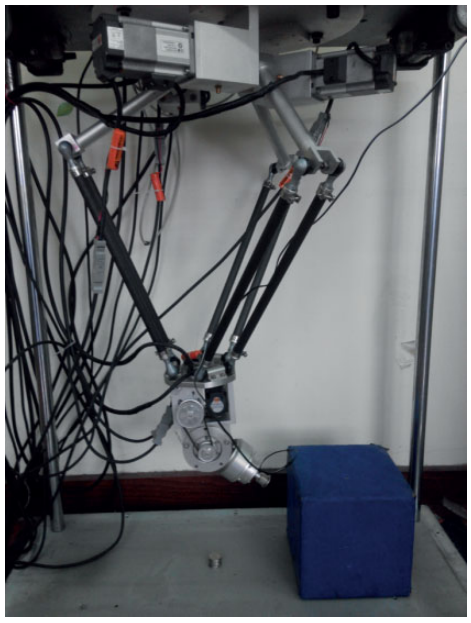

Figure 2. The five-DOF hybrid robot. 5-DOF: five-degrees-of-freedom.

section, the mechanism of the five-DOF hybrid robot is introduced as follows. The five-DOF hybrid robot consists of a base, a movable platform, three drive arms, three follower arms, and a two-DOF serial mechanism. The parallel part of the robot can achieve three translational movements by three identical branches. Each branch has a drive arm and a follower arm. The mechanical model of the hybrid robot is shown in Figure 1(a). The mechanism of the swing and rotation is installed on the moveable platform. The AC servo motor, the harmonic reducer, and the synchronous belt are used to achieve high positioning precision. Bevel gears are adopted to realize the rotation of the end effector. The hybrid robot is shown in Figure 2.

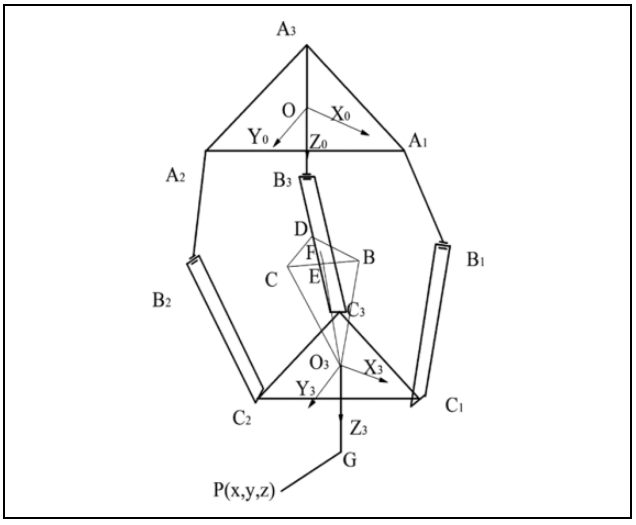

Figure 3. The mechanism sketch of the robot.

As a delta robot, the moveable platform can achieve three translational movements. As shown in Figure 1(b), with the fourth swing axis, the end effector can swing back and forth. With the fifth rotation axis, the end effector can rotate around its own axis. The work space is largely expanded by the two joints. The five-DOF hybrid robot combines the advantages of parallel robot and serial robot and has potential application in many fields.

Kinematics analysis

The kinematics analysis is a fundamental work in the modeling of the five-DOF hybrid robot.[14] The kinematics of the robot includes forward kinematics and the inverse kinematics. Forward kinematics analysis is calculating the position and attitude of the end effector according to the geometric parameters and joint angles. Inverse kinematics analysis is calculating the joint angles according to the position and posture of the end effector. The kinematics analysis can lay the foundation of control and future optimization.

Forward kinematics

The forward kinematics of the five-DOF hybrid robot consists of the parallel part and the serial part. First, the parallel mechanism kinematics is solved. As described in Figure 3, a straight line O_3B is parallel to B_1C_1, a straight line O_3C is parallel to O_2C_2, and a straight line O_3D is parallel to B_3C_3. Let $\boldsymbol{O_3B} = \boldsymbol{B_1C_1}$, $\boldsymbol{O_3C} = \boldsymbol{B_2C_2}$, and $\boldsymbol{O_3D} = \boldsymbol{B_3C_3}$. Thus, we get the new triangular pyramid $O_3 - BCD$. The coordinates of vertex O_3 can be solved according to the levers' length

$$\boldsymbol{OB_1} = \boldsymbol{OA_1} + \boldsymbol{A_1B_1}$$
$$\boldsymbol{OB_2} = \boldsymbol{OA_2} + \boldsymbol{A_2B_2}$$
$$\boldsymbol{OB_3} = \boldsymbol{OA_3} + \boldsymbol{A_3B_3}$$

$$\boldsymbol{OB} = \boldsymbol{OB_1} + \boldsymbol{B_1B} = \boldsymbol{OB_1} + \boldsymbol{A_1O}$$
$$\boldsymbol{OD} = \boldsymbol{OB_3} + \boldsymbol{B_3D} = \boldsymbol{OB_3} + \boldsymbol{A_3O}$$

Then, we consider triangular pyramid $O_3 - BCD$. E is the midpoint of side BC. F is the projection of point O_3 in the surface BCD. It can be proved that F is the circumcenter of BCD, so

$$\boldsymbol{OO_3} = \boldsymbol{OF} + \boldsymbol{FO_3}$$
$$\boldsymbol{OF} = \boldsymbol{OE} + \boldsymbol{EF}$$

where, $\boldsymbol{OE} = (\boldsymbol{OB} + \boldsymbol{OC})/\boldsymbol{2}, \boldsymbol{EF} = |\boldsymbol{EF}| \cdot \boldsymbol{n_{EF}}, |\boldsymbol{EF}|$ refers to the unit vector along EF

$$\boldsymbol{n_{EF}} = \frac{\boldsymbol{BC} \times \boldsymbol{CD} \times \boldsymbol{BC}}{|\boldsymbol{BC}||\boldsymbol{CD}||\boldsymbol{BC}|\sin\frac{\pi}{3}}$$

$$|\boldsymbol{EF}| = \sqrt{|\boldsymbol{BF}|^2 - |\boldsymbol{BE}|^2}$$

where, $\boldsymbol{BE} = \frac{\boldsymbol{BC}}{2}$

$$|\boldsymbol{BF}| = \frac{|\boldsymbol{BC}||\boldsymbol{CD}||\boldsymbol{BD}|}{4\sqrt{p(p - |\boldsymbol{BC}|)(p - |\boldsymbol{CD}|)(p - |\boldsymbol{BC}|)}}$$

Similarly, vector $\boldsymbol{FA}$ can be solved by

$$\boldsymbol{FO_3} = |\boldsymbol{FO_3}|\boldsymbol{n_{FO_3}}$$

where

$$|\boldsymbol{FO_3}| = \sqrt{|\boldsymbol{O_3B}|^2 - |\boldsymbol{BF}|^2}$$
$$\boldsymbol{n_{FO_3}} = \frac{\boldsymbol{BC} \times \boldsymbol{CD}}{|\boldsymbol{BC}||\boldsymbol{CD}|\sin\frac{\pi}{3}}$$

So far, $\boldsymbol{OF}$ and $\boldsymbol{OF_3}$ can be obtained. While $\boldsymbol{OO_3} = \boldsymbol{OF} + \boldsymbol{FO_3}$, the coordinates of point O_3 can be calculated. O_3 is denoted by (x_0, y_0, z_0). Then the coordinates of end effector $P(x, y, z)$ can be calculated by

$$\begin{cases} x = x_0 \\ y = y_0 + L_5 \sin\theta_4 \\ z = z_0 + L_4 + L_5 \cos\theta_4 \end{cases}$$

where L_4 refers to the length of lever O_3G and L_5 refers to the length of lever GP.

Inverse kinematics

Considering the special structure of delta robots, inverse kinematics methods mainly include geometry method and D-H matrix method.[15–17] D-H matrix method is used for inverse kinematics analysis. Before the analysis, we need to build the relative coordinate system between the connecting levers. As the three connecting levers involved in the robot are identical, we only need to analyze one branch of them. The coordinate system is shown in Figure 4. As can

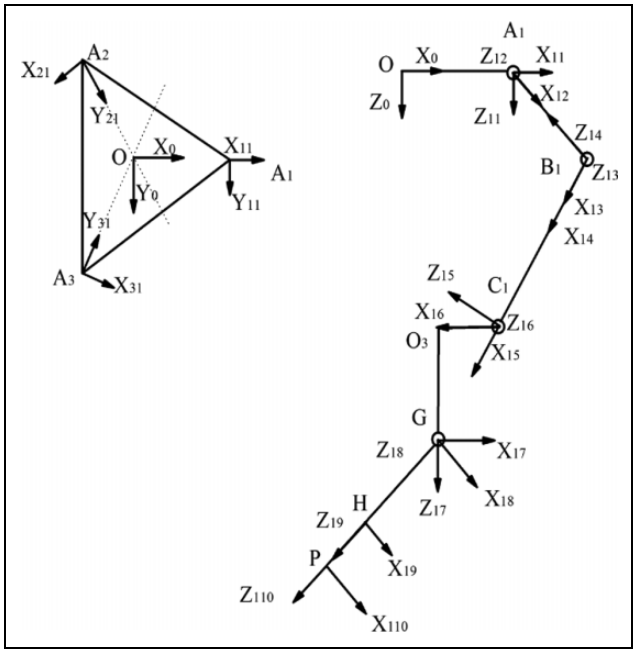

Figure 4. The coordinates system of the robot.

be seen in Figure 4, $O - x_0y_0z_0$ is the world coordinate system. $O - x_{110}y_{110}z_{110}$ is the end coordinate system. For the hybrid robot, $O_1A = R$, $O_3C_1 = r$, $A_1B_1 = L_1$, $B_1C_1 = L_2$, $O_3G = L_3$, $GH = L_4$, $HP = L_5$. According to D-H matrix method, link transform ${}_i^{i-1}T$ depends on four parameters a_{i-1}, α_{i-1}, d_i, and θ_i. The transform ${}_i^{i-1}T$ can be decomposed into four basic self-transform problems which are rotation α_{i-1} around x_{i-1} axis, translation a_{i-1} along x_{i-1} axis, rotation θ_i around $z_i - 1$ axis, and translation d_i along z_{i-1} axis. According to from left to right principle, we can get

$$ {}_i^{i-1}T = \text{Screw}(x, a_{i-1}, \alpha_{i-1})\ \text{Screw}(z, d_i, \theta_i) $$

where $\text{Screw}(k, a, \alpha)$ refers to the translation a along k axis, rotation α around k axis. So we can get general formula

$$ {}_i^{i-1}T = \begin{pmatrix} c\theta_i & -s\theta_i & 0 & a_{i-1} \\ s\theta_i c\alpha_{i-1} & c\theta_i c\alpha_{i-1} & -s\alpha_{i-1} & -d_i s\alpha_{i-1} \\ s\theta_i s\alpha_{i-1} & c\theta_i c\alpha_{i-1} & c\alpha_{i-1} & d_i c\alpha_{i-1} \\ 0 & 0 & 0 & 1 \end{pmatrix} \tag{1} $$

where $c\theta_i$ refers to $\cos\theta_i$, $s\theta_i$ refers to $\sin\theta_i$, Multiplying ${}_i^{i-1}T(i = 1, 2, \ldots, n)$, we get

$$ {}_n^0T = {}_1^0T\,{}_2^1T{}_3^2T \cdots {}_n^{n-1}T \tag{2} $$

where ${}_n^0T$ is the arm transformation matrix. It is a function of n variables. The variables are listed in Table 1.

According to parameters in Table 1, we get the distal coordinates as follows

$$ {}_{10}^0T = {}_1^0T\,{}_2^1T \cdots {}_{10}^9T \tag{3} $$

Table 1. The link parameters of 5-DOF hybrid robot.

No.	a_{i-1}	α_{i-1}	d_i	θ_i
1	R	0	0	0
2	0	90°	0	θ_2
3	L_1	0	0	θ_3
4	0	−90°	0	θ_4
5	L_2	0	0	θ_5
6	0	90°	0	θ_6
7	r	90°	L_3	π
8	0	90°	0	θ_8
9	0	−90°	L_4	θ_9
10	0	0	L_5	0

5-DOF: five-degrees-of-freedom.

The end effector of the robot can move along the X, Y, and Z directions, can rotate around Y axis, and can rotate around the output shaft. The homogeneous transformation matrix of point G is shown below

$$ G = \begin{pmatrix} 1 & 0 & 0 & m \\ 0 & 1 & 0 & n \\ 0 & 0 & 1 & q \\ 0 & 0 & 0 & 1 \end{pmatrix} \tag{4} $$

The homogeneous transformation matrix of point P is

$$ P = \begin{pmatrix} \cos\theta_y\cos\theta & -\cos\theta_y\sin\theta & -\sin\theta & x \\ \sin\theta & \cos\theta & 0 & y \\ \sin\theta_y\cos\theta & -\sin\theta_y\sin\theta & -\cos\theta_y & z \\ 0 & 0 & 0 & 1 \end{pmatrix} \tag{5} $$

where $[x, y, z]$ is the position coordinates of point P in the coordinate system $O - xyz$.θ_y is the swing angle around Y axis in coordinate system $O - xyz$. θ is the rotation angle around the output shaft of the robot. $[m, n, q]$ is the position coordinates of the point D in the coordinate system $O - xyz$. According to equation (2)

$$ {}_7^0T = {}_1^0T\,{}_2^1T \cdots {}_7^6T \tag{6} $$

By equations (3) to (6)

$$ {}_{10}^0T = P \tag{7} $$

$$ {}_7^0T = D \tag{8} $$

The inverse kinematics is to calculate the robot joint angle according to the position and posture of the end effector. For the hybrid robot, the inverse kinematics is to calculate $[\theta_2, \theta_3, \theta_4, \theta_5, \theta_6, \theta_8, \theta_9]$ using $[x, y, z, \theta_y, \theta]$. Using the inverse kinematics method proposed by Paul, we premultiplicate equation (1) by unknown link inverse transformation. By separating joint variables, we can get solution. Because the corresponding items on both sides of equation (8) are equal, the following result can be obtained

$$ \theta_8 = \theta_y, \theta_9 = \theta $$

By equations (6) and (8)

$$P = D_8^7 T_9^8 T_{10}^9 T \tag{9}$$

$$\begin{cases} x = m - (L_4 + L_5)\cos\theta_8 \\ y = n \\ z = q + (L_4 + L_5)\sin\theta_8 \end{cases} \tag{10}$$

$${}_7^0T = \begin{pmatrix} n_x & o_x & a_x & m \\ n_y & o_y & a_y & n \\ n_z & o_z & a_z & q \\ 0 & 0 & 0 & 1 \end{pmatrix} \tag{11}$$

where

$$n_x = s(\theta_2 + \theta_3)s\theta_6 - c(\theta_2 + \theta_3)c(\theta_4 + \theta_5)c\theta_6$$

$$n_y = -s(\theta_4 + \theta_5)c\theta_6$$

$$n_z = -c(\theta_2 + \theta_3)s\theta_6 - s(\theta_2 + \theta_3)c(\theta_4 + \theta_5)c\theta_6$$

$$o_x = -c(\theta_2 + \theta_3)s(\theta_4 + \theta_5)$$

$$o_y = c(\theta_4 + \theta_5)$$

$$o_z = -s(\theta_2 + \theta_3)s(\theta_4 + \theta_5)$$

$$a_x = s(\theta_2 + \theta_3)c\theta_6 + c(\theta_2 + \theta_3)c(\theta_4 + \theta_5)s\theta_6$$

$$a_y = s(\theta_4 + \theta_5)s\theta_6$$

$$a_z = c(\theta_4 + \theta_5)s(\theta_2 + \theta_3)s\theta_6 - c(\theta_2 + \theta_3)c\theta_6$$

$$m = R + L_1c\theta_2 + L_3a_x - rn_x + L_2c(\theta_2 + \theta_3)c\theta_4$$

$$n = L_2s\theta_4 + rs(\theta_4 + \theta_5)c\theta_6 + L_3s(\theta_4 + \theta_5)s\theta_6$$

$$q = L_1s\theta_2 + L_3a_z + rn_z + L_2s(\theta_2 + \theta_3)c\theta_4$$

Thus, from equation (8), we get $n_x = 1, o_y = 1$, namely

$$\begin{cases} s(\theta_2 + \theta_3)s\theta_6 - c(\theta_2 + \theta_3)c(\theta_4 + \theta_5)c\theta_6 = 1 \\ c(\theta_4 + \theta_5) = 1 \end{cases} \tag{12}$$

Solving equations

$$\begin{cases} \theta_2 + \theta_3 + \theta_4 = \pi \\ \theta_4 + \theta_5 = 0 \end{cases} \tag{13}$$

Then, substituting m, n, q and equation (13) into equation (10), we have

$$\begin{cases} R + L_1c\theta_2 - r - L_2c\theta_6c\theta_4 = x + (L_4 + L_5)\cos\theta_8 \\ L_2s\theta_4 = y \\ L_3 + L_1s\theta_2 + L_2s\theta_6c\theta_4 = z - (L_4 + L_5)\sin\theta_8 \end{cases} \tag{14}$$

Solving equations, the driving angle θ_2 should be

$$\theta_2 = \arcsin\frac{tt_1 + \sqrt{(tt_1)^2 - (t_1^2 + t_2^2)(t^2 - t_1^2)}}{t_1^2 + t_2^2} \tag{15}$$

where

$$t_1 = x + (L_4 + L_5)\cos\theta_8 + R - r$$

$$t_2 = z - (L_4 + L_5)\sin\theta_8 - L_3$$

$$t = t_1\cos\theta_6 - t_2\sin\theta_6$$

So far, the joint angles of the branch have been solved. The joint angles of the other two branches can be calculated in the same way.

Dynamics model

In this section, the dynamic model of the hybrid robot is derived by using the Lagrange formulation and energy method. Suppose that the Cartesian coordinates are used to describe the location of the components. The position and the attitude R, γ, q of the end effector should be

$$R = [x, y, z]^T, \gamma = [\psi, \theta, \phi]^T, q = [R^T, \gamma^T]$$

The transformation matrix from centroid coordinates to reference coordinates can be expressed as

$$A = \begin{pmatrix} c\psi c\phi - s\psi c\theta s\phi & -c\psi s\psi - s\psi c\theta c\phi & s\psi s\theta \\ s\psi c\phi + c\psi c\theta s\phi & -s\psi s\phi + c\psi c\theta c\phi & -c\psi s\theta \\ s\theta s\phi & s\theta c\phi & c\theta \end{pmatrix} \tag{16}$$

Suppose that the Euler angles coordinates are used to reflect the components movement. The transformation matrix from rotation coordinates to centroid coordinates should be expressed as follows

$$A = \begin{pmatrix} \sin\theta\sin\phi & 0 & \cos\theta \\ \sin\theta\cos\phi & 0 & -\sin\theta \\ \cos\theta & 1 & 0 \end{pmatrix} \tag{17}$$

The principle of virtual work states that a system of rigid bodies is in dynamic equilibrium when the virtual work of the sum of the applied forces and the inertial forces is 0 for any virtual displacement of the system. Thus, dynamic equilibrium can be written as

$$\delta W = (Q_1 + Q_1^*)\delta W q_1 + \cdots + (Q_n + Q_n^*)\delta q_n = 0$$

The n equations can be written in differential form

$$\frac{d}{dt}\frac{\partial T}{\partial \dot{q}_j} - \frac{T}{q_j} = Q_j, j = 1, \cdots, n \tag{18}$$

Based on the principle of virtual work, the Lagrange equation can be established as

$$\frac{d}{dt}\frac{\partial T}{\partial \dot{q}_j} - \frac{\partial T}{\partial q_j} = Q_j + \sum_{i=1}^{n}\lambda_i\frac{\partial \Phi}{\partial q_j} \tag{19}$$

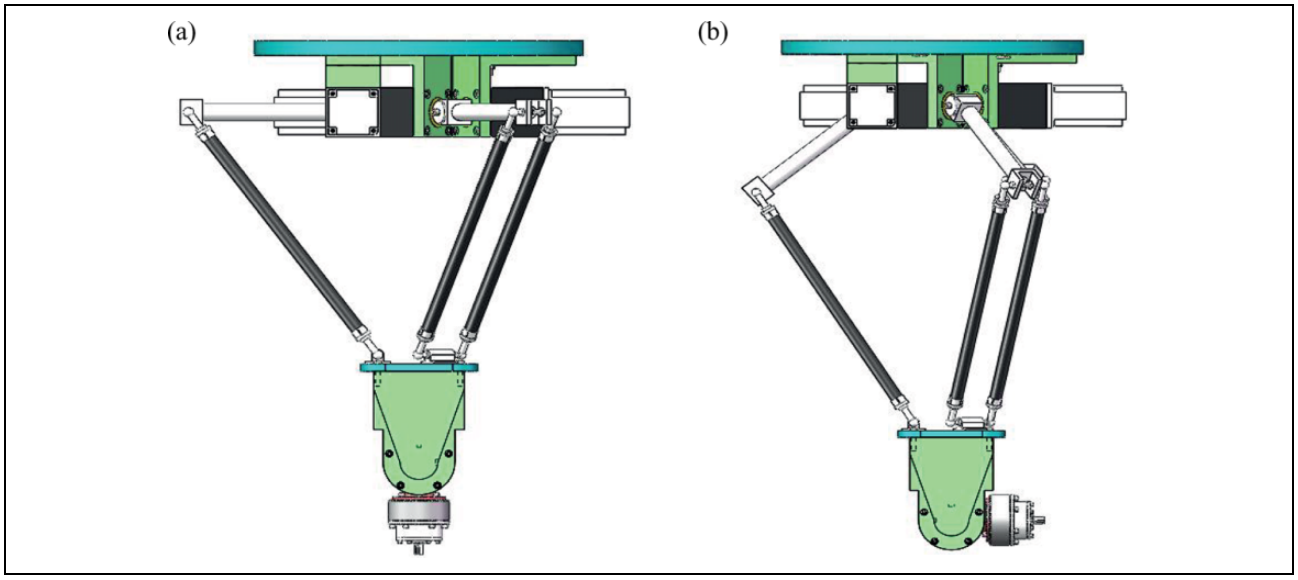

Figure 5. The dynamics simulation model: (a) the initial posture and (b) the final posture.

The Lagrange equation can be simplified as

$$\dot{P}_j - \frac{\partial T}{\partial q_j} = Q_j - C_j \tag{20}$$

where the kinetic energy T can be expressed as

$$T = \frac{1}{2}\dot{R}^T M\dot{R} + \frac{1}{2}\dot{\gamma}^T B^T JB\dot{\gamma} \tag{21}$$

Equation (20) can be decomposed into translation equation (22) and rotation equation (23)

$$\dot{P}_R - \frac{\partial T}{\partial q_R} = Q_R - C_R \tag{22}$$

$$\dot{P}_\gamma - \frac{\partial T}{\partial q_\gamma} = Q_\gamma - C_\gamma \tag{23}$$

Thus, the motion equation of each component can be acquired

$$\begin{cases} M\dot{V} = Q_R - C_R \\ V = \dot{R} \\ \dot{P}_\gamma - \dfrac{\partial T}{\partial q_\gamma} = Q_\gamma - C_\gamma \\ P_\gamma = \dfrac{\partial T}{\partial q_\gamma} = B^T JB\omega_e \\ \omega_\varepsilon = \dot{\gamma} \end{cases} \tag{24}$$

where

$$V = [V_x, V_y, V_z]^T$$

$$R = [x, y, z]^T$$

$$P_\gamma = [P_\psi, P_\theta, P_\phi]$$

$$\omega_e = [\omega_\psi, \omega_\theta, \omega_\phi]^T$$

$$\gamma = [\psi, \theta, \phi]^T$$

Then, the dynamic equations of hybrid robot should be

$$\begin{cases} \dot{P} - \dfrac{\partial T}{\partial q} + \Phi_q^T \lambda + H^T F = 0 \\ P = \dfrac{\partial T}{\partial \dot{q}} \\ u = \dot{q} \\ \Phi(q, t) = 0 \\ F = f(u, q, t) \end{cases} \tag{25}$$

Dynamics simulation

In order to verify the dynamics performance of the hybrid robot, the dynamic simulation is carried out by the ADAMS and SolidWorks analysis tools. The model of hybrid robot is built in SolidWorks, and then, it is imported into ADAMS. Since the 3-D model of hybrid robot is too complex, we need to simplify the model by removing the less important components and combine some relatively static parts as a whole. The simplification can increase the running speed in ADAMS. After the preprocessing, we can do the simulation. Let hybrid robot run from the initial position to the final position. The gesture is shown in Figure 5.

The model runs from the initial position to the final position in 0.5 s. The torque of key joints is shown in Figure 6. The angles of key joints are shown in Figure 7. The velocity of end actuator is shown in Figure 8. Through the simulation, we can get the torque, the velocity, and the

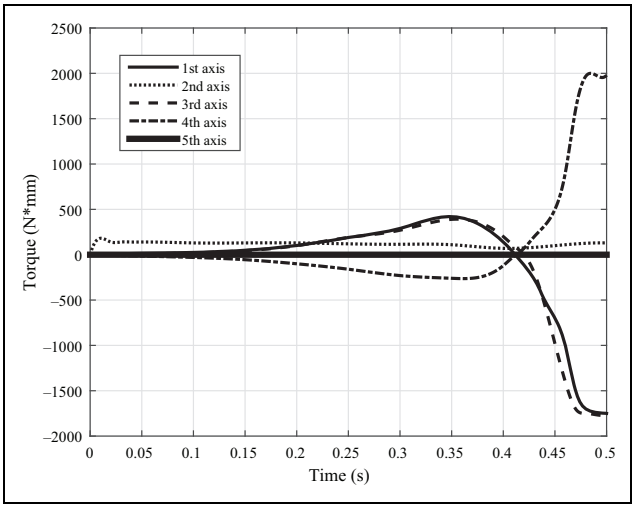

Figure 6. The torque curves of each axis.

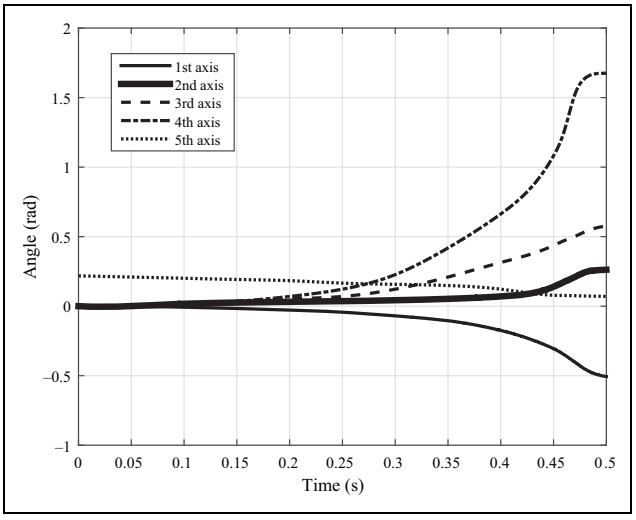

Figure 7. The angle curves of each axis.

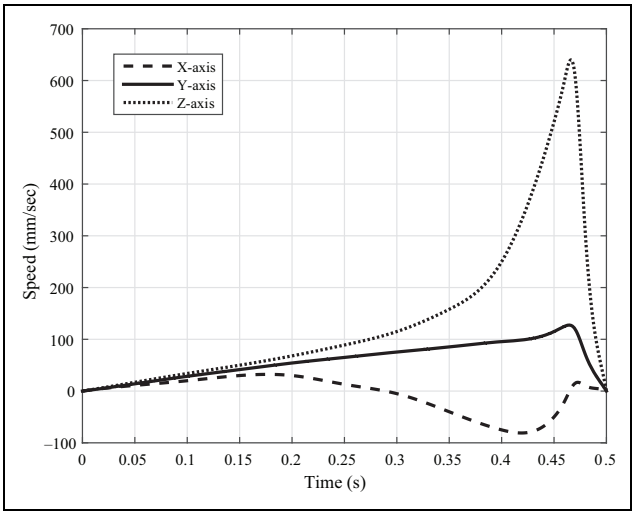

Figure 8. The speed of the end effector.

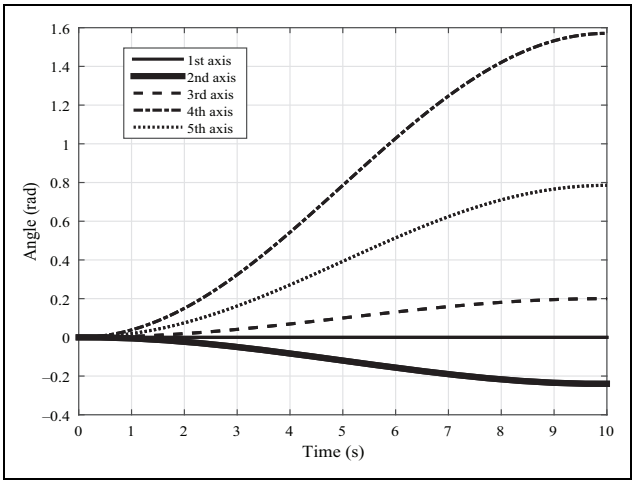

Figure 9. The angle curves of each axis.

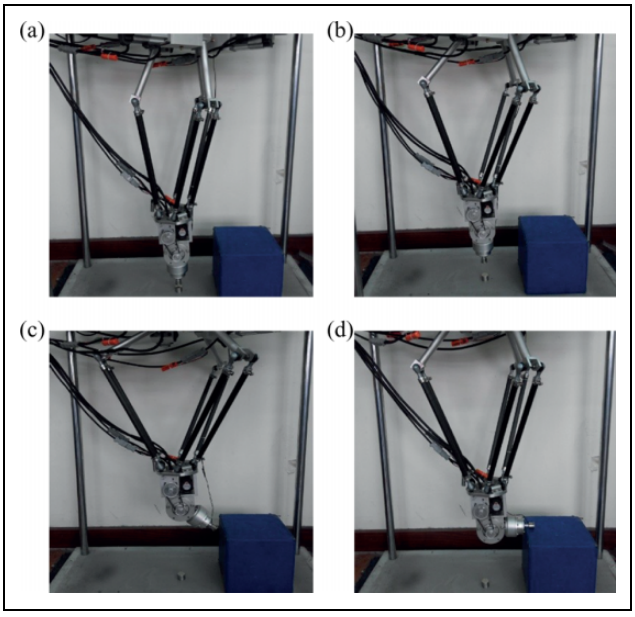

Figure 10. The experiment process.

angle of each joint. From Figures 6 to 8, we can see that the hybrid robot can move from 0 to 600 mm/s in 0.5 s, and maxim torque of the joint can reach 2 Nm and more. The dynamic simulation shown that the five-DOF hybrid robot has robust dynamic performance.

Experiment

After kinematics calculations and trajectory planning, the picking up and placing experiments are carried out to verify the feasibility and accuracy of the hybrid robot. In the experiments, an electromagnet is mounted as the end effector to do the picking up and placing task. The coins are used as the workpieces to be picked up from one place to another.

For the hybrid robot, $R = 100$ mm, $r = 50$ mm, $L_1 = 350$ mm, $L_2 = 700$ mm, $L_3 = 140$ mm, $L_4 = 30$ mm,

$L_5 = 50$ mm. The position and attitude of the end effector can be defined as $P(x, y, z, \alpha, \beta)$. The end effector moves from one point $P_1 = (0, 0, -500, 0, 0)$ to another point $P_2(50, 200, -800, \frac{\pi}{2}, \frac{\pi}{4})$. The inverse kinematics calculation and the trajectory planning are carried out by the control system of the hybrid robot. The eight-axes PMAC motion control card is adopted as the open control platform. The trajectory planning curve of each axis is shown in Figure 9.

In the experiment, the electromagnet successfully picked up the coins from one place to another with the accuracy of 0.1 mm. The process is given in Figure 10. The results shown that the hybrid robot can meet the requirement of the picking up application. The five-DOF hybrid robot also has a potential application of the assembly for its flexible ability.

Conclusion

A novel five-DOF hybrid robot is proposed in this article. Based on the delta robot, the hybrid robot consists of a base, a movable platform, three drive arms, three follower arms, and a serial mechanism. The robot has three translational DOFs and two rotational DOFs. The forward kinematics is derived by the geometry method, and the inverse kinematics is derived by the D-H matrix method. Then the dynamics models are constructed through Lagrange formulation. The dynamics simulation is carried out by ADAMS software. In the simulation, the hybrid robot runs from the initial position to the final position. The torque curves of each axis, the angle curves of each curves, and the speed of the end effector are obtained. The analysis results will lay the foundation of future application. At last, the experiment shows the feasibility of the hybrid robot applying in the basic picking and placing operation.

Declaration of conflicting interests

The author(s) declared no potential conflicts of interest with respect to the research, authorship, and/or publication of this article.

Funding

The author(s) disclosed receipt of the following financial support for the research, authorship, and/or publication of this article: This work is partially supported by the National Natural Science Foundation of China and National Basic Research Program of China (grant nos. U1401240, 2014CB046302, 61473192, and 61075086). Research Project supported by Shanghai Committee of Science and Technology, China (grant no. 17441901000).

References

1. Gallardo J, Lesso R, Rico JM, et al. The kinematics of modular spatial hyper-redundant manipulators formed from RPS-type limbs. *Robot Auton Syst* 2011; 59(1): 12–21.
2. Hu B and Yu J. Unified solving inverse dynamics of 6-DOF serialCparallel manipulators. *Appl Math Model* 2015; 39(16): 4715–4732.
3. Kelaiaia R, Zaatri A, and Chikh L. Some investigations into the optimal dimensional synthesis of parallel robots. *Int J Adv Manuf Technol* 2016; 83(9–12): 1525–1538.
4. Tsai LW and Joshi S. Kinematic analysis of 3-DOF position mechanisms for use in hybrid kinematic machines. *J Mech Des* 2002; 124(2): 245–253.
5. Tsai CY, Wong CC, Yu CJ, et al. A hybrid switched reactive-based visual servo control of 5-DOF robot manipulators for pick-and-place tasks. *IEEE Syst J* 2015; 9(1): 119–130.
6. Romdhane L. Design and analysis of a hybrid serial-parallel manipulator. *Mech Mach Theory* 1999; 34(7): 1037–1055.
7. Fan C, Zhao G, Zhao J, et al. Calibration of a parallel mechanism in a serial-parallel polishing machine tool based on genetic algorithm. *Int J Adv Manuf Technol* 2015; 81(1–4): 27–37.
8. Huang T, Li M, Zhao XM, et al. Conceptual design and dimensional synthesis for a 3-DOF module of the TriVarianta novel 5-DOF reconfigurable hybrid robot. *IEEE Trans Robot* 2005; 21(3): 449–456.
9. Liang C and Ceccarelli M. Design and simulation of a waist-Ctrunk system for a humanoid robot. *Mech Mach Theory* 2012; 53: 50–65.
10. Liang C, Ceccarelli M, and Carbone G. Experimental characterization of operation of a waist-trunk system with parallel manipulators. *Chin J Mech Eng* 2011; 24(5): 713–722.
11. Poppeova V, Uríček J, Bulej V, et al. Delta robots–robots for high speed manipulation. *Tehnicki vjesnik* 2011; 18(3): 435–445.
12. Carp-Ciocardia DC. Dynamic analysis of Clavel's delta parallel robot. In: *IEEE international conference on robotics and automation*, Taipei, Taiwan IEEE Xplore, NY, USA, 14–19 September 2003, Vol. 3, pp. 4116–4121. IEEE.
13. Featherstone R and Orin D. Robot dynamics: equations and algorithms. In: *Proceeding IEEE International Conference Robotics & Automation*, San Francisco, CA, USA, 24–28 April 2000.
14. Peidro A, Gil A, Marin JM, et al. Inverse kinematic analysis of a redundant hybrid climbing robot. *Int J Adv Robot Syst* 2015; 12(11): 163.
15. Kvrgic VM, Visnjic ZM, Cvijanovic VB, et al. Dynamics and control of a spatial disorientation trainer. *Robot Comput Integr Manuf* 2015; 35: 104–125.
16. Wei H, Yuanying Q, and Jian Y. An approach to evaluate stability for cable-based parallel camera robots with hybrid tension-stiffness properties. *Int J Adv Robot Syst* 2015; 12: 1.
17. Cheng H, Yiu YK, and Li Z. Dynamics and control of redundantly actuated parallel manipulators. *IEEE/ASME Trans Mech* 2003; 8(4): 483–491.